Preliminary Results Toward a Naturally Controlled Multi-Synergistic Prosthetic hand.

Matteo Rossi[1,2], Cosimo Della Santina[2], Cristina Piazza[2],
Giorgio Grioli[1], Manuel Catalano[1], Antonio Bicchi[1,2]

Abstract— increasing interest thanks to their simplicity and robustness, combined with good performances. Another key aspect of these hands is that humans can use them very effectively thanks to the similarity of their behavior with natural ones. Nevertheless, controlling more than a degree of actuation remains a challenging task.

In this paper we move a first step in taking advantage of such characteristics in a multi-synergistic prosthesis. We propose an integrated setup comprehending Pisa/IIT SoftHand 2 robotic hand and a control strategy which simultaneously and proportionally maps the human hand movements to the robotic hand. The control technique is based on a combination of non-negative matrix factorization and linear regression algorithms. It also features a real-time continuous posture compensation of the electromyographic signals based on an IMU. The algorithm is tested on five healthy subjects through a virtual reality experiment. In a separate experiment, the efficacy of the posture compensation strategy is evaluated on five subjects and, finally, the whole setup is successfully tested in performing realistic daily life activities.

I. INTRODUCTION

State of the art robotic and prosthetic hands are still far from bridging the gap with the human hand. The biomechanical complexity together with the advanced skills of the human sensory-motor system represent a big challenge for the development of new mechatronic solutions capable of the simultaneous, proportional and fluid movements and interactions that the human hand is capable of. To try filling this gap, two main trends of research animate robotic hand design. On one side many hands are designed trying to match the many functions of human hands through a complex design, including sophisticated combinations of several motors and sensors. Noteworthy examples are [1][2]. Typically these hands have the drawbacks of being expensive and fragile. Furthermore the problem of controlling them is in general very complex because of the large number of inputs that have to be regulated. This makes them very hard to control for a human operator [3][4].

To overcome these limitations, other hands proposed in literature aim at embedding some functional principles into their mechanics [5][6]. Among the main tools of this research

[1]Department of Advanced Robotics, Istituto Italiano di Tecnologia, Genoa, Italy

[2]Centro di Ricerca "E. Piaggio", Universita di Pisa, Largo L. Lazzarino, 1, 56126 Pisa, Italy.
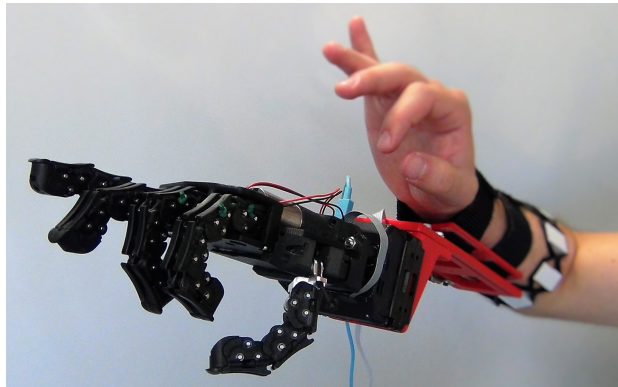
Correspond to: matteo.rossi at iit.it

Fig. 1.   Pisa/IIT SoftHand 2 controlled though MYO armband.

approach are under-actuation [7], compliant mechanics [8], and a human-aware approach to the system design [9]. Thanks to this approach, it is possible to design hands able to cope with part of the problem complexity directly at the mechanical level. It results in a strong simplification of their design, such as of the associated control interface.

Pisa/IIT SoftHand+ is an heavily under-actuated robotic hand [10], and it is an evolution of the Pisa/IIT SoftHand [11]. It implements two degrees of actuation, inspired by the most common human hand postures (namely postural hand synergies) as found in [12] and [13]. It is the authors opinion that the reduced dimension of the actuation space, combined with the human inspiration, should make this class of under-actuated and soft hands valuable candidate not only for use on autonomous robotic manipulators (as e.g. [14], [15]) but also for applications where a human user is active part of the planning and control loop, spanning from tele-operation, to prosthetics, to human grasp studies and rehabilitation robotics. Preliminary results in this sense with Pisa/IIT SoftHand are provided in [16] [17].

Here we discuss the application of Pisa/IIT SoftHand 2 (Fig. 1), an evolution of Pisa/IIT SoftHand+ [10], to the previously discussed fields. To moving a first step in the direction of advancing Pisa/IIT SoftHand 2 into a prosthetic hand, it would be very useful to simplify as much as possible the interface it presents to a human operator, making it intuitive to use.

In this paper we face this problem by proposing and implementing a novel control algorithm that takes advantages from the most recent trends in myo-electric control (state of the art is discussed in Sec. II). The controller implemented

in this work is a combination of linear regression (LR) and non-negative matrix factorization (NMF). Furthermore we propose to use the arm posture acquired through an IMU, to compensate the artifacts found in electromyographic (EMG) signals due to limb position [18]. While other works have investigated the use of IMU data to increase the accuracy of classifiers [19] [20], to the best of the our knowledge this is the first study that investigates the use of an IMU to directly compensate the EMG signals. The algorithm is implemented so as to function with a low cost myo-electric off-the-shelf input device, the Myo Armband, from Thalmic Labs [21].

Various experimental results are provided in order to demonstrate the effectiveness of the whole system, including a quantitative study of the algorithm in a real-time virtual environment with five subjects, and a qualitative study where an operator intuitively executes a set of realistic daily life activities.

The paper is organized as follows: Sec. III introduces Pisa/IIT SoftHand 2 and the problem of its control, while Sec. IV presents the control algorithm. In Sec. V the experiments are described, provided and discussed. Sec. VI presents the results. Finally conclusions are drawn in Sec. VII.

II. STATE OF THE ART

Myoelectric interfaces have in fact been widely used to control assistive devices, in particular for the control of upper-limb prostheses. However, myoelectric control of multiple degrees of freedom in a simultaneous way remains an open problem. The control strategy typically implemented in multi-DOF prostheses consists in the proportional control of a single DOF at a time with the possibility of switching between DOFs by a co-contraction signal. In the attempt to control multiple DOFs without the need for switching, a vast variety of classification-based approaches have been proposed [22].

Despite the good performances in classifying and control reached by these methods, they have the strong limitation in terms of naturalness of control. In fact natural movements that involve two or more DOFs should be obtained by controlling the joints simultaneously and proportionally, but a classifier can only detect one function at time. By enriching the training set, it was shown that it is possible to achieve the simultaneous activation of multiple classes [23]; however, this approach can lead to a deterioration of classification accuracy and more complicated training sessions. For this reason we focus our attention on a different class of control algorithms.

The use of regression techniques is an interesting alternative to the classification approach. These methods have been successfully applied to the simultaneous and proportional control of multiple DOFs, e.g. artificial neural networks (ANN) in [24], linear regression (LR) in [25] and non-negative matrix factorization (NMF) in [26].

Among the regression methods for EMG control, NMF presents several advantages. Besides being computationally efficient and requiring little user training, the non-negativity of the NMF approaches is in agreement with the fact that the firing rates of motor neurons can either increase or decrease but must always remain positive [27]. Also, it has been shown that the online performance of NMF is generally comparable or better than ANN and LR [28].

During preliminary tests with NMF, however, the authors noticed that when a subject had to perform movements characterized by a high intensity of the muscular activity in the attempt of activating one DOF in a certain direction, the component related to the same DOF, but with opposite direction, was often activated as well, thus limiting the range of the control signals. In the attempt of solving this issue, a new control algorithm, based on the union of NMF and LR, was developed. The proposed algorithm also encompass a mechanism of real-time compensation of the EMG signals through posture information.

III. PROBLEM DEFINITION & SETUP

Following the principle introduced in [10], SoftHand 2 is actuated with a transmission system encompassing just one tendon, pulleys and two motors, each end of the actuation tendon is pulled by one of the two motors. Fig. 2(a) presents a sketch of SoftHand 2 , with the two motors underlined. SoftHand 2 inherits good grasping skills from Pisa/IIT SoftHand with which share the first degree of actuation. Furthermore thanks to the novel degree of actuation Pisa/IIT SoftHand 2 can reach particularly useful postures, Fig. 2(b) shows some of them. In the center of the figure is reported the hand rest position, and along the two axis are presented the postures resulting from the application of the two degrees of actuation. For further details on SoftHand 2 structure we refer to future works.

If adopted on a robot manipulator the SoftHand 2 can be controlled simply through an external digital input by computer, anyway if the goal is to use the hand in applications such as ones described in Sec. I the problem of controlling the hand becomes much more complex. To test the Pisa/IIT SoftHand the operator interface was a dedicated handle, as shown in Fig. 3 (a), maneuvered by the operator by strapping it to their arm and controlled via the clenching of the user fist around a hand-lever 3(b). This interface demonstrated to be very easy and intuitive. We observe that this could be due to the fact that the user operates the handle lever with a motion that is somehow similar to the first grasp synergy that the SoftHand implements as its degree of actuation. The problem of controlling the SoftHand 2 is more complex because of the device nature, in fact in order to operate two synergies, two different commands have to be generated. A similar approach, with a mechanical handle could be implemented with the Pisa/IIT SoftHand 2, as shown in Fig.3(c), but the intuitiveness of the system is lower w.r.t. the solution adopted for the Pisa/IIT SoftHand. The ideal, most intuitive control interface should, in principle, extract the projection of the user hand motion along the two synergies corresponding to those actuated by the SoftHand 2 and then map these two values into actual commands to the robot hand (as it was explored in [17] for the control of the first synergy of the
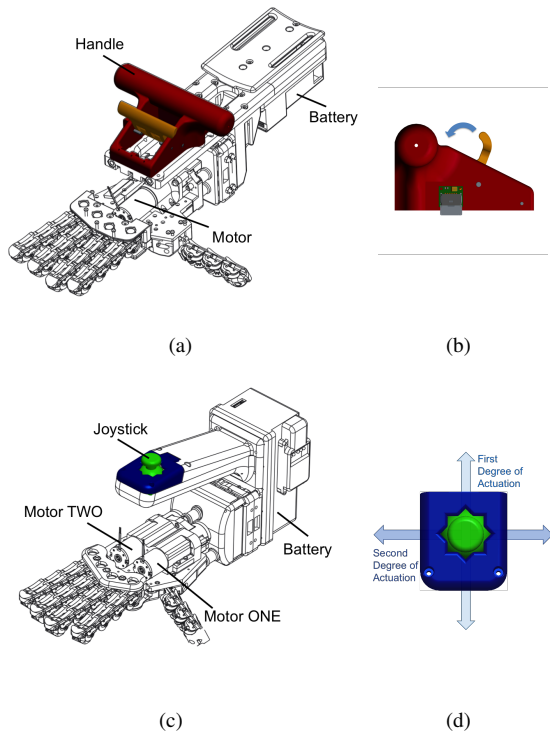
(a)

(b)

(c)

(d)

Fig. 3. CAD model of Pisa/IIT SoftHand (a) and of Pisa/IIT SoftHand2 (c) mounted on their handles. Note that the handle (a) is operated by clenching a hand-lever (b), with a movement similar to that of the first synergy, while (c) is controlled using a joystick (d).

SoftHand). This mapping does not need to be very strict, as operator's brain plasticity is likely to compensate minor deviations, but a substantial amount of similarity eases the operator task of controlling a system [29], [30].

Fig. 4 presents the whole setup, composed by the robotic hand Pisa/IIT SoftHand 2 , the EMG system Myo armband, and a mechanical interface used to connect the robotic hand to the operator's arm. Myo armband, by Thalmic Labs, is a wearable device that features eight stainless steel EMG sensors and a nine-axis IMU, which consists of a three-axis accelerometer, a three-axis gyroscope, and a three-axis magnetometer. The EMG signals are sampled at a frequency of 200Hz, while the sampling frequency for the IMU data is 50Hz. The acquired data is streamed to a computer via Bluetooth communication. The choice of this device was driven by (i) the portability of the device and (ii) the on-board inclusion of an IMU, taking also in consideration its relatively low cost. The device embeds also a vibro-tactile feedback device that the authors aim to integrate in the testing framework in the near future.

In this work, the Myo armband is wore by each subject around the thickest part of the right forearm (approximately in the first proximal third of the forearm) where the electrodes can sense the activity of the main extrinsic hand muscles.
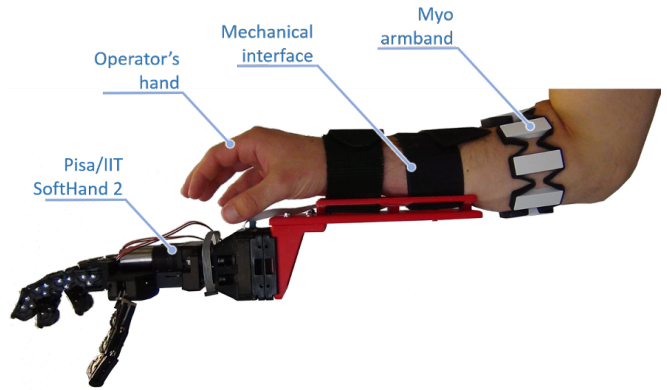

Fig. 4. Considered setup, composed by the Pisa/IIT SoftHand 2 , the mechanical interface to connect it to the user arm, and the Myo armband.

IV. CONTROL ALGORITHM

A. EMG Filtering and Posture Compensation

We will consider in the following 8 normalized EMG signals $q_i, i \in \{1 \ldots 8\}$ acquired at 200Hz from the operator forearm, as depicted in Fig. 4 and described in Sec. III. The mean absolute value (MAV) of such signals is defined as

$$q_{f,i}(t) = \frac{1}{N} \sum_{k=t-N+1}^{t} |q_i(k)|, \qquad (1)$$

where N is number of samples in the moving window and $q_{f,i}(t)$ is the MAV of q_i at time t. In this work, a moving window with $N = 40$ (200ms) is used.

In order to avoid undesired movement of the robotic hand when changing forearm posture with respect to gravity, a posture compensation technique was applied to the EMG signals. Note that along with the normalized EMG signals, Myo Armband also provides the asset, in the form of quaternions, of the sensor frame $\mathscr{F}'$ with respect to an inertial reference frame $\mathscr{F}$. The angle γ between the Z axis of $\mathscr{F}'$ (forearm longitudinal axis, pointing proximally) and the Z axis of $\mathscr{F}$ (vertical axis with opposite direction with respect to gravity) is computed from the quaternion readings.

From the training data, an average μ_i of each filtered EMG signal $q_{f,i}$ is computed in 2 different postures: $\gamma = 0$ and $\gamma = \frac{\pi}{2}$, only for the values that correspond to a resting phase. Thus we propose here the following simple real-time compensation rule for the signals $q_{f,i}$

$$q_{c,i}(t) = \begin{cases} x_i(t), & \text{if } x_i(t) \geq 0 \\ 0, & \text{if } x_i(t) < 0 \end{cases} \qquad i = 1, \ldots, 8, \qquad (2)$$

where $x_i(t)$ is

$$x_i(t) = q_{f,i}(t) + (\cos \gamma(t) - 1) \frac{\mu_{i,\gamma=0}}{\mu_{i,\gamma=1}}. \qquad (3)$$

Two examples of compensated signals are shown in Fig. 5. The compensated (in red) and non compensated (in blue) EMG signals from two different sensors are relative to the repetition of the same gesture in different orientations of the forearm. While the EMG activity detected by sensor 1 is not

(a) Pisa/IIT SoftHand 2

First Degree of Actuation

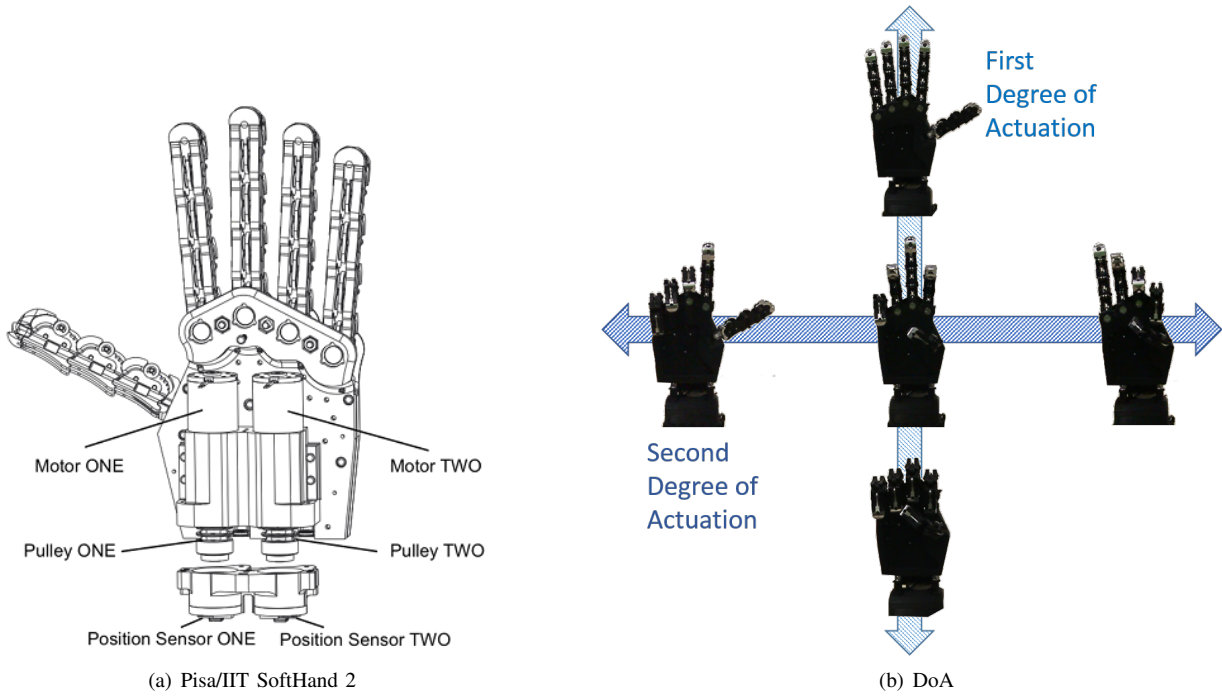Second Degree of Actuation

(b) DoA

Fig. 2. (a) presents a sketch of Pisa/IIT SoftHand 2 with its two motors. (b) shows a representation of Pisa/IIT SoftHand 2 closures correspondent to the two degree of actuations (DoA). In the middle of the figure we report the hand rest position. The other four configurations are the extreme postures obtainable through one of the two degrees of actuations. All the linear combinations of these two degrees are achievable by the hand.
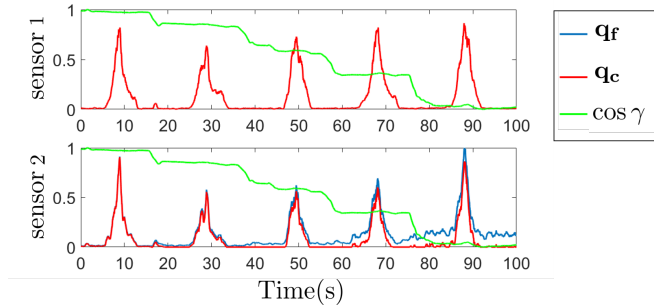

Fig. 5. Compensated (q_c) and non compensated (q_f) EMG signals acquired from two sensors during the repetition of the same hand gesture in different postures (increasing values of γ).

affected by the changes in posture, and thus the compensated and non compensated signals coincide, when $\cos\gamma$ (shown in green) is close to 0, sensor 2 is detecting EMG activity during rest phases that may cause unwanted activations of the robotic hand, thus the compensation is desirable.

B. NMF

Non-negative matrix factorization (NMF) is a method for the factorization of a matrix $\mathbf{A} \in \mathbb{R}^{m \times T}$, into two matrices $\mathbf{S} \in \mathbb{R}^{m \times n}$ and $\mathbf{U} \in \mathbb{R}^{n \times T}$, with the requirement that the three matrices, $\mathbf{A}$, $\mathbf{S}$ and $\mathbf{U}$, can only have non-negative entries, i.e. $\mathbf{A} \approx \mathbf{SU}$.

The elements of $\mathbf{S}$ and $\mathbf{U}$ can be determined by optimizing an error function J between $\mathbf{A}$ and $\mathbf{SU}$. The most commonly used cost function J is

$$J = ||\mathbf{A} - \mathbf{SU}||_2, \qquad (4)$$

where $||\cdot||_2$ denotes the 2-norm.

This optimization problem can be solved using a supervised approach [27] that exploits information on the intended movement during the training phase allows more robust and repeatable results. The matrix A is defined as

$$\mathbf{A} = \begin{bmatrix} a_1(0) & \cdots & a_1(T) \\ \vdots & \ddots & \vdots \\ a_m(0) & \cdots & a_m(T) \end{bmatrix}, \qquad (5)$$

where the activation level for each movement, $a_k(t)$ with $k \in \{1 \dots m\}$, is described by a value comprised between 0 (relaxed state) and 1 (maximum intensity), and represents the activation intensity of movement k that is requested to the user during the training phase at the time instant t. Four different control movements ($m = 4$) are used, which correspond to two different directions for each degree of freedom.

The matrix $\mathbf{S}$ can be used to find an estimate of the activation intensity $\hat{\mathbf{a}}(t)$ by computing the product with the MAV of the filtered EMG signals (vector $\mathbf{u}(t)$)

$$\hat{\mathbf{a}}(t) = \begin{bmatrix} s_{1,1} & \cdots & s_{1,8} \\ \vdots & \ddots & \vdots \\ s_{4,1} & \cdots & s_{4,8} \end{bmatrix} \mathbf{u}(t) = \mathbf{S}\mathbf{u}(t) \qquad (6)$$

To obtain the two control signals needed, $y_1(t)$ and $y_2(t)$, it is then sufficient to find, for each degree of freedom, the difference of the activation intensities that correspond to opposite directions

$$\mathbf{y}(t) = \begin{bmatrix} y_1(t) \\ y_2(t) \end{bmatrix} = \begin{bmatrix} 1 & 0 & -1 & 0 \\ 0 & 1 & 0 & -1 \end{bmatrix} \mathbf{S}\mathbf{u}(t) \qquad (7)$$

C. NMF + LR

The NMF method previously described was compared to a cascade of NMF and LR. In particular, two regression models were trained for each DOF, for a total of four models. The models were trained on the output of the NMF algorithm

$$\hat{\mathbf{a}}'(t) = \mathbf{B^T S u}(t) + \mathbf{A_0}, \qquad (8)$$

where $\hat{\mathbf{a}}'(t)$ is the vector of the estimated activation levels for the four movements at the instant t, $\mathbf{B} \in \mathbb{R}^{mxm}$ contains the weight vectors and $\mathbf{A_0}$ is the constant offset that was set to zero. Given a training-set composed of T time instances, the entries of $\mathbf{B}$ were found by solving the equation

$$\mathbf{B} = (\mathbf{SUU^T S^T})^{-1} \mathbf{SUA^T}. \qquad (9)$$

Once the elements of $\mathbf{B}$ are found, the product $\mathbf{B^T S}$ can be calculated offline during the training phase and the new estimate $\hat{\mathbf{a}}'(t)$ can be computed in real-time with no additional computational cost with respect to $\hat{\mathbf{a}}(t)$.
Similarly to the previous case, to obtain the two control signals needed it is sufficient to find, for each degree of freedom, the difference of the activation intensities that correspond to opposite directions

$$\mathbf{y}(t) = \begin{bmatrix} y_1(t) \\ y_2(t) \end{bmatrix} = \begin{bmatrix} 1 & 0 & -1 & 0 \\ 0 & 1 & 0 & -1 \end{bmatrix} \mathbf{B^T S u}(t). \quad (10)$$

V. EXPERIMENTS

To test the effectiveness of the implemented algorithm, three different test were performed by naive subjects. The first test is the target acquisition experiment, to assess and compare NMF and the here proposed NMF+LR. Then the balance experiment was execute, for the posture compensation. Finally, a qualitative test was purpose to investigate the method performing daily activity tasks. Each subject provided written informed consent.

A. Target Acquisition Experiment

To compare NMF and NMF+LR performances within the here proposed setup, five subjects performed a target acquisition task in a virtual reality environment. The control signals extracted by the EMGs were used to control the position of a cursor (a blue sphere) on the screen (see Fig. 6). The subjects were asked to reach a fixed target, represented by a red sphere, as quickly as possible, and to keep the blue sphere on the target until disappearance. After 500 consecutive milliseconds in which the two spheres overlapped, the target was considered acquired and the red sphere disappeared. If the target was not acquired during the first $10s$, the attempt was regarded as a failure and the red sphere disappeared. After a target disappeared, another target appeared after $4s$ of rest. The targets were placed at $0, \frac{\pi}{8}, \frac{2\pi}{8}, \dots, \frac{15\pi}{8}$ and presented in random order. The distance of the targets from the center was set respectively to 50%, 75% and 100% of the total range during three different trials for each algorithm. The six trials were scattered and presented in a different order to each subject. To assess the performance of the subjects, four outcome measures
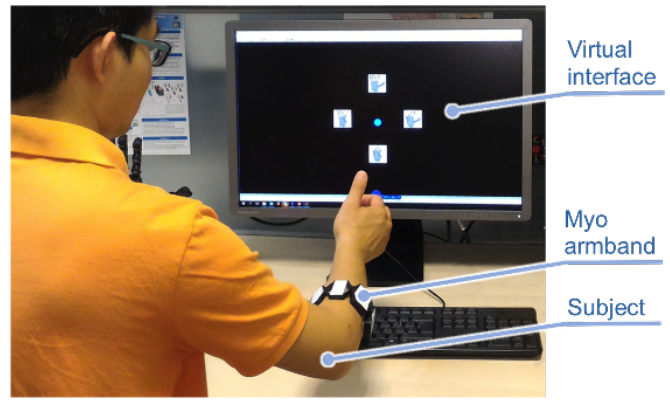

Fig. 6. Setup used for target acquisition experiment. The virtual interface consists of four hand posture representation and a target (represented by a blue sphere) that moves randomly between the hand postures. Each subject was asked to follow the moving target. During the experiment the subject was wearing a MYO armband.

as described in [24][31] were used: *acquisition rate*, *path efficiency*, *completion time* and *overshoot*.

B. Balance Experiment

A balance experiment was also performed by five subjects to assess the performance of the EMG compensation strategy. The whole setup was wore on the subjects' right forearm using the wearable mechanical interface of Fig. 4. The subjects were asked to perform the training procedure for the control algorithm two times, keeping the forearm horizontal ($\gamma = \frac{\pi}{2}$) and vertical ($\gamma = 0$) respectively. The parameters for the compensation were then extracted as described in IV-A. Using the virtual reality environment previously described, the control signals extracted by the EMGs were again mapped to the position of the cursor. The control range was mapped to a circular area of radius 1 on the screen.
Prior to the test, it was verified that the subjects were able to perform the main movements at full range (positions $(0,1)$, $(1,0)$, $(0,-1)$ and $(-1,0)$ on the screen), keeping the forearm in three different orientations ($\gamma \approx 0$, $\gamma \approx \frac{\pi}{4}$ and $\gamma \approx \frac{\pi}{2}$), and both with posture compensation ON and OFF.
The test consisted in keeping the cursor in the origin (relaxed state) for 5 consecutive seconds, with the forearm respectively in $\gamma \approx 0$, $\gamma \approx \frac{\pi}{4}$ and $\gamma \approx \frac{\pi}{2}$ conditions, and without the aid of visual feedback. As a performance metric, the average distance of the cursor from the origin was used, being 0 the ideal result, and 1 the worst case.

C. Qualitative Test

One subject participated in the qualitative test. The subject had prior experience with myo-electric control. The experiment consisted of three phases: training, practice and test. During the first phase, the NMF+LR algorithm was trained and the parameters for the EMG compensation were extracted.
During the second phase, the subject was given some time to practice with the control interface and with the SoftHand 2. During the test, the subject was presented with some realistic

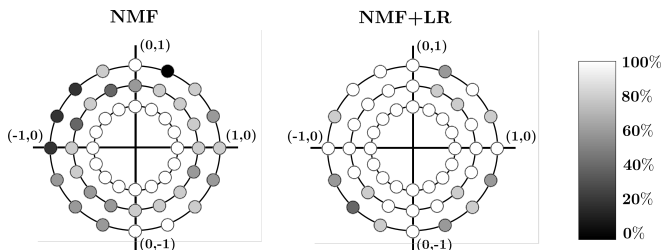|	NMF	NMF + LR	p-Value
Acquisition rate (%)	77.08 ± 0.13	92.08 ± 5.39	0.02
Path efficiency (%)	43.16 ± 6.54	44.63 ± 5.99	> 0.1
Completion time (s)	2.68 ± 0.30	2.17 ± 0.10	0.04
Overshoot	0.55 ± 0.28	0.61 ± 0.10	> 0.1

Fig. 7. Graphical representation of the average *acquisition rate* for each target. Each dot represents a target and its color represents the number of times that the target was acquired, from 0% of the times (dark red) to 100% of the times (dark green).

tasks and was let free to accomplish them in the way he considered the most efficient. The tasks were focused on activity of daily living and bi-manual coordination. The tasks included grasping a banknote, switching the lights off, firmly grasping a hammer, placing an egg in an egg carton, grasping an apple and extracting a credit card from a wallet.

VI. RESULTS

A. Target Acquisition Experiment

Table I summarizes the performance of the control schemes during the target acquisition task, for the various performance metrics, averaged across all users. The NMF+LR method outperformed the NMF method in terms of *acquisition rate* ($p = 0.02$), and produced significantly lower *completion time* ($p = 0.04$). No significant difference was found in terms of *path efficiency* and NMF performed slightly better in terms of *overshoot* with respect to NMF+LR, although the difference was not statistically significant ($p > 0.1$).

Fig. 7 illustrates the average *acquisition rate* for each target. Each dot represents a target and its color represents the number of times that the target was acquired, from 0 (dark red) to 5 (dark green). All of the targets that were at a distance of 50% of the total range from the origin were acquired by all subjects for both conditions (NMF and NMF+LR). For further targets (with a distance of 75% and 100% of the total range from the origin), the NMF+LR method had better performance for almost all directions.

B. Balance Experiment

The results of the balance experiment are shown in Table II. When the forearm was kept in a vertical position ($\gamma \approx 0$), the average distance between the cursor and the origin was kept low ($< 10\%$ of the total range) for both the compensated

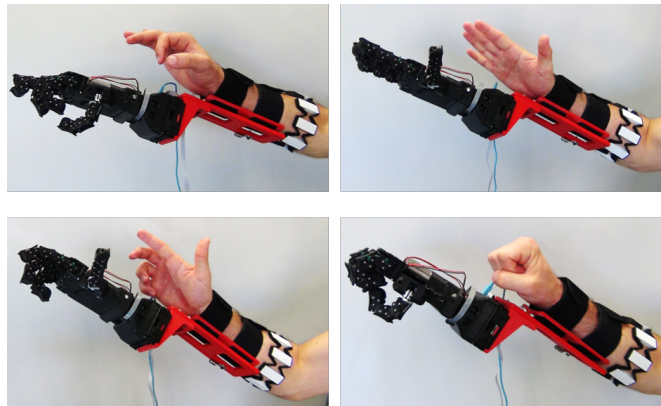|	Compensation OFF	Compensation ON	p-Value
case $\gamma \approx 0$	0.06 ± 0.03	0.05 ± 0.03	> 0.1
case $\gamma \approx \frac{\pi}{4}$	0.15 ± 0.05	0.05 ± 0.02	0.03
case $\gamma \approx \frac{\pi}{2}$	0.25 ± 0.05	0.03 ± 0.02	0.01

Fig. 8. Representation of Pisa/IIT SoftHand 2 closures correspondent to the two DoA.

and the non-compensated conditions. No statistical difference between the two conditions was found in this case ($p > 0.1$). In the other conditions, i.e. when the forearm was kept respectively at a $45°$ angle ($\gamma \approx \frac{\pi}{4}$) and $0°$ angle ($\gamma \approx \frac{\pi}{2}$) from the horizontal plane, the non-compensated condition resulted in higher distances of the cursor from the origin (respectively $> 10\%$ and $> 20\%$ of the total range), while the compensated condition resulted in low distances (10% of the total range) for all cases, outperforming the non-compensated condition.

C. Qualitative Test

Fig. 8 shows how the proposed strategy achieve the goal stated in Sec. III: the operator hand posture is naturally mapped into the robotic hand on the four postures of Fig. 2(b). Fig. 9 and 10 show the execution of some of the tasks during the qualitative test. In particular, in Fig. 9 are displayed two different closures to accomplish the same task in different ways: grasping a banknote. After experimenting two different grasps, a power grasp and a pinch grasp, the subject chose the latter as best suited for picking up thin and deformable objects such as banknotes. As shown in Fig.10, during the test the subject was able to successfully switch buttons (a), grasp heavy objects (b), manipulate fragile objects (c) and grasp objects and moving the arm without dropping them (d). Also complete bi-manual tasks (an examples is shown in Fig. 11) were successfully performed. Additional examples can be found on the video attachment.
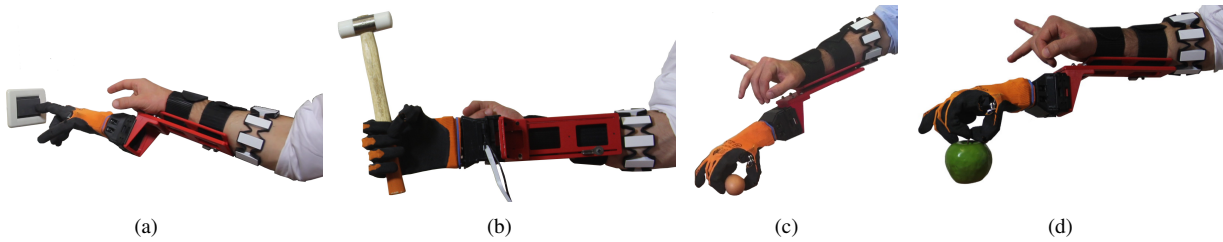
Fig. 10. Some examples of grasps using different postures of the Pisa/IIT Softhand 2: switch buttons (a), grasp heavy objects (b), manipulate fragile objects (c) and grasp objects and moving the arm without dropping them (d).

Fig. 11. Bi-manual task consist of open a wallet and grasp a credit card performed by switching between different postures of the hand.

Fig. 9. An example of power and pinch grasp of a banknote. The similarity between the posture of an operator's hand and the Pisa/IIT SoftHand 2 highlights the simplicity of this control strategy.

VII. DISCUSSION & CONCLUSIONS

In this paper, the online performance of two control algorithms based respectively on NMF and NMF+LR regression techniques, were compared in order to choose a suitable candidate for the control of the SoftHand 2. The choice of using online vs offline performance was motivated by the literature: it has been in fact shown that the offline performance of a myoelectric control algorithm has little predictive value with respect to its online control performance [24] [28]. A target acquisition test, widely employed in myoelectric control, was chosen for the performance assessment in order to facilitate comparative analyses with similar studies. Four performance metrics were computed for the evaluation of the control quality: *acquisition rate*, *path efficiency*, *completion time* and *overshoot*.

The *acquisition rate* obtained with the NMF algorithm was significantly lower than some results presented in the literature [27][32][33]. A difference in performance could be due to the hardware used to acquire the EMG signals; the cheap and off-the-shelf sensors used in this paper are of course less precise than far more expensive acquisition systems normally used in laboratories. Also, the choice of the movements was motivated by the control intuitiveness of

the SoftHand 2 instead of opting for more recognizable and less intuitive movements such as wrist movements [27][32] [33]. However, the same conditions applied to the NMF+LR algorithm, which performed significantly better. It is the opinion of the authors that this difference was partially due to the difficulties encountered by the subjects when using the NMF algorithm to control the cursor at the range limits. This hypothesis is supported by the results shown in Fig. 7, where it can be seen that the major difference in performance between the NMF and the NMF+LR concerns the targets positioned at a distance equal to 100% of the motion range. Given its superior performance in the target acquisition task, the NMF+LR algorithm was selected for the following experiments.

While most research concerning myoelectric control algorithms is done in a laboratory, with stable conditions, the ultimate goal for these interfaces is to be used in a real environment for activities of daily living, with far less stable conditions. One of the factors that is for instance seldom taken into account is the variability of the EMG signals due to changes in arm posture [34] [35]. In this paper, a strategy to compensate for the influence of static postures on EMG signals was implemented. The results of the balance experiment showed that when the compensation strategy was active, it allowed the subjects to maintain a *rest* command to the robotic hand while keeping their hand at rest in different positions. On the other hand, when the compensation strategy was not active, on average, unwanted commands as big as 25% of the total control range were generated by the subjects while keeping their hand at rest.

Finally the whole setup was also successfully tested by a healthy subject for the control of the SoftHand 2 in a realistic scenario to perform daily life activities. This new system will enable exploring the possibility of using the SoftHand 2 in various fields as tele-operation, assistive robotics and prosthetics. The investigation of all these possibilities is

ongoing work carried on by the authors.

REFERENCES

[1] M. Grebenstein, A. Albu-Schäffer, T. Bahls, M. Chalon, O. Eiberger, W. Friedl, R. Gruber, S. Haddadin, U. Hagn, R. Haslinger *et al.*, "The dlr hand arm system," in *Robotics and Automation (ICRA), 2011 IEEE International Conference on*. IEEE, 2011, pp. 3175–3182.

[2] A. Kochan, "Shadow delivers first hand," *Industrial robot: an international journal*, vol. 32, no. 1, pp. 15–16, 2005.

[3] J. T. Belter, J. L. Segil, and B. SM, "Mechanical design and performance specifications of anthropomorphic prosthetic hands: a review," *Journal of rehabilitation research and development*, vol. 50, no. 5, p. 599, 2013.

[4] C. Piazza, C. Della Santina, M. Catalano, G. Grioli, M. Garabini, and A. Bicchi, "Softhand pro-d: Matching dynamic content of natural user commands with hand embodiment for enhanced prosthesis control," in *Robotics and Automation (ICRA), 2016 IEEE International Conference on*. IEEE, 2016, pp. 3516–3523.

[5] L. U. Odhner, L. P. Jentoft, M. R. Claffee, N. Corson, Y. Tenzer, R. R. Ma, M. Buehler, R. Kohout, R. D. Howe, and A. M. Dollar, "A compliant, underactuated hand for robust manipulation," *The International Journal of Robotics Research*, vol. 33, no. 5, pp. 736–752, 2014.

[6] R. Deimel and O. Brock, "A novel type of compliant and underactuated robotic hand for dexterous grasping," *The International Journal of Robotics Research*, p. 0278364915592961, 2015.

[7] L. Birglen, T. Laliberté, and C. M. Gosselin, *Underactuated robotic hands*. Springer, 2007, vol. 40.

[8] A. Albu-Schaffer, O. Eiberger, M. Grebenstein, S. Haddadin, C. Ott, T. Wimbock, S. Wolf, and G. Hirzinger, "Soft robotics," *IEEE Robotics & Automation Magazine*, vol. 15, no. 3, pp. 20–30, 2008.

[9] A. Bicchi, M. Gabiccini, and M. Santello, "Modelling natural and artificial hands with synergies," *Philosophical Transactions of the Royal Society B: Biological Sciences*, vol. 366, no. 1581, pp. 3153–3161, 2011.

[10] C. Della Santina, G. Grioli, M. Catalano, A. Brando, and A. Bicchi, "Dexterity augmentation on a synergistic hand: The pisa/iit softhand+," in *Humanoid Robots (Humanoids), 2015 IEEE-RAS 15th International Conference on*. IEEE, 2015, pp. 497–503.

[11] M. G. Catalano, G. Grioli, E. Farnioli, A. Serio, C. Piazza, and A. Bicchi, "Adaptive synergies for the design and control of the pisa/iit softhand," *The International Journal of Robotics Research*, vol. 33, no. 5, pp. 768–782, 2014.

[12] M. Santello, M. Flanders, and J. F. Soechting, "Postural hand synergies for tool use," *The Journal of Neuroscience*, vol. 18, no. 23, pp. 10 105–10 115, 1998.

[13] M. Gabiccini, G. Stillfried, H. Marino, and M. Bianchi, "A data-driven kinematic model of the human hand with soft-tissue artifact compensation mechanism for grasp synergy analysis," in *Intelligent Robots and Systems (IROS), 2013 IEEE/RSJ International Conference on*. IEEE, 2013, pp. 3738–3745.

[14] F. Negrello, M. Garabini, M. G. Catalano, P. Kryczka, W. Choi, D. Caldwell, A. Bicchi, and N. Tsagarakis, "Walk-man humanoid lower body design optimization for enhanced physical performance," in *Robotics and Automation, 2016. ICRA'16. IEEE International Conference on*, 2016.

[15] A. Ajoudani, J. Lee, A. Rocchi, M. Ferrati, E. M. Hoffman, A. Settimi, D. G. Caldwell, A. Bicchi, and N. G. Tsagarakis, "A manipulation framework for compliant humanoid coman: Application to a valve turning task," in *2014 IEEE-RAS International Conference on Humanoid Robots*. IEEE, 2014, pp. 664–670.

[16] S. B. Godfrey, A. Ajoudani, M. G. Catalano, G. Grioli, and A. Bicchi, "A synergy-driven approach to a myoelectric hand," in *13TH International Conference on Rehabilitation Robotics*, June 24-26, 2013, Seattle, WA., 2013, pp. 1 – 6. [Online]. Available: 10.1109/ICORR.2013.6650377

[17] A. Brygo, I. Sarakoglou, A. Ajoudani, N. Hernandez, G. Grioli, M. Catalano, D. Caldwell, and N. Tsagarakis, "Synergy-based interface for bilateral tele-manipulations of a master-slave system with large asymmetries."

[18] R. N. Khushaba, A. Al-Timemy, S. Kodagoda, and K. Nazarpour, "Combined influence of forearm orientation and muscular contraction on emg pattern recognition," *Expert Systems with Applications*, vol. 61, pp. 154–161, 2016.

[19] A. Fougner, E. Scheme, A. D. Chan, K. Englehart, and Ø. Stavdahl, "Resolving the limb position effect in myoelectric pattern recognition," *IEEE Transactions on Neural Systems and Rehabilitation Engineering*, vol. 19, no. 6, pp. 644–651, 2011.

[20] M. T. Wolf, C. Assad, M. T. Vernacchia, J. Fromm, and H. L. Jethani, "Gesture-based robot control with variable autonomy from the jpl biosleeve," in *Robotics and Automation (ICRA), 2013 IEEE International Conference on*. IEEE, 2013, pp. 1160–1165.

[21] Myo Armband, "https://www.myo.com/."

[22] M. A. Oskoei and H. Hu, "Myoelectric control systemsa survey," *Biomedical Signal Processing and Control*, vol. 2, no. 4, pp. 275–294, 2007.

[23] A. J. Young, L. H. Smith, E. J. Rouse, and L. J. Hargrove, "Classification of simultaneous movements using surface emg pattern recognition," *IEEE Transactions on Biomedical Engineering*, vol. 60, no. 5, pp. 1250–1258, 2013.

[24] A. Ameri, E. N. Kamavuako, E. J. Scheme, K. B. Englehart, and P. A. Parker, "Real-time, simultaneous myoelectric control using visual target-based training paradigm," *Biomedical Signal Processing and Control*, vol. 13, pp. 8–14, 2014.

[25] J. Hahne, F. Biessmann, N. Jiang, H. Rehbaum, D. Farina, F. Meinecke, K.-R. Müller, and L. Parra, "Linear and nonlinear regression techniques for simultaneous and proportional myoelectric control," *IEEE Transactions on Neural Systems and Rehabilitation Engineering*, vol. 22, no. 2, pp. 269–279, 2014.

[26] N. Jiang, K. B. Englehart, and P. A. Parker, "Extracting simultaneous and proportional neural control information for multiple-dof prostheses from the surface electromyographic signal," *IEEE Transactions on Biomedical Engineering*, vol. 56, no. 4, pp. 1070–1080, 2009.

[27] C. Choi and J. Kim, "Synergy matrices to estimate fluid wrist movements by surface electromyography," *Medical engineering & physics*, vol. 33, no. 8, pp. 916–923, 2011.

[28] N. Jiang, I. Vujaklija, H. Rehbaum, B. Graimann, and D. Farina, "Is accurate mapping of emg signals on kinematics needed for precise online myoelectric control?" *IEEE Transactions on Neural Systems and Rehabilitation Engineering*, vol. 22, no. 3, pp. 549–558, 2014.

[29] X. Liu, K. M. Mosier, F. A. Mussa-Ivaldi, M. Casadio, and R. A. Scheidt, "Reorganization of finger coordination patterns during adaptation to rotation and scaling of a newly learned sensorimotor transformation," *Journal of neurophysiology*, vol. 105, no. 1, pp. 454–473, 2011.

[30] D. J. Berger, R. Gentner, T. Edmunds, D. K. Pai, and A. d'Avella, "Differences in adaptation rates after virtual surgeries provide direct evidence for modularity," *The Journal of Neuroscience*, vol. 33, no. 30, pp. 12 384–12 394, 2013.

[31] M. R. Williams and R. F. Kirsch, "Evaluation of head orientation and neck muscle emg signals as command inputs to a human–computer interface for individuals with high tetraplegia," *IEEE Transactions on Neural Systems and Rehabilitation Engineering*, vol. 16, no. 5, pp. 485–496, 2008.

[32] J. M. Hahne, S. Dähne, H.-J. Hwang, K.-R. Müller, and L. C. Parra, "Concurrent adaptation of human and machine improves simultaneous and proportional myoelectric control," *IEEE Transactions on Neural Systems and Rehabilitation Engineering*, vol. 23, no. 4, pp. 618–627, 2015.

[33] N. Jiang, H. Rehbaum, I. Vujaklija, B. Graimann, and D. Farina, "Intuitive, online, simultaneous, and proportional myoelectric control over two degrees-of-freedom in upper limb amputees," *IEEE transactions on neural systems and rehabilitation engineering*, vol. 22, no. 3, pp. 501–510, 2014.

[34] J. C. Jamison and G. E. Caldwell, "Muscle synergies and isometric torque production: influence of supination and pronation level on elbow flexion," *Journal of neurophysiology*, vol. 70, no. 3, pp. 947–960, 1993.

[35] J. Howard, J. D. Hoit, R. Enoka, and Z. Hasan, "Relative activation of two human elbow flexors under isometric conditions: a cautionary note

concerning flexor equivalence," *Experimental brain research*, vol. 62, no. 1, pp. 199–202, 1986.